Int. J. Heat Mass Transfer. Vol. 25, No. 9, pp. 1343–1351, 1982
Printed in Great Britain

0017-9310/82/091343-09 $03.00/0
Pergamon Press Ltd.

A METHOD OF PREDICTING THE 'DIAMETER EFFECT' FOR HEAT TRANSFER AND FRICTION OF DRAG-REDUCING FLUIDS

E. F. MATTHYS and R. H. SABERSKY
California Institute of Technology, Pasadena, CA 91125, U.S.A.

(*Received* 29 *March* 1982)

Abstract—A multilayered velocity profile has been assumed to exist for 'drag reducing' fluids flowing in a pipe. The profile is characterized by a logarithmic portion offset by an increment Δu^+ from that pertaining to a Newtonian fluid. For a given fluid Δu^+ is assumed to be determined by the shear velocity u_τ. On this basis a method is proposed by which one may predict the effect of changes in diameter on the friction and heat transfer coefficients.

NOMENCLATURE

- A, intersection point of viscous and asymptotic layers (Fig. 3);
- B, intersection point of asymptotic and logarithmic layers (Fig. 3);
- C, concentration of solution [ppm];
- C_F, friction coefficient, $\tau_w/[(\rho u_m^2)/2]$;
- C_H, heat transfer coefficient, $q_w/[\rho C_p u_m(T_w - T_m)]$;
- C_p, specific heat [J kg^{-1} K^{-1}];
- D, pipe diameter [m];
- k, thermal conductivity [W m^{-1} K^{-1}];
- P, parameter characterizing the nature of the solution;
- Pr, Prandtl number evaluated at T_m, $(\mu C_p)/k$;
- Pr_ε, 'turbulent' Prandtl number, $(\nu + \varepsilon_M)/(\alpha + \varepsilon_H)$;
- q, heat flux [W m^{-2}];
- q_w, heat flux at wall [W m^{-2}];
- R, pipe radius [m];
- R^+, dimensionless radius, $(Ru_\tau)/\nu$;
- Re, Reynolds number, $(u_m D)/\nu$;
- T, temperature [K];
- T^+, dimensionless temperature, $(T\rho C_p u_\tau)/q_w$;
- T_m, average temperature in pipe [K];
- T_w, wall temperature [K];
- T_m^+, dimensionless average temperature, $(T_m \rho C_p u_\tau)/q_w$;
- T_w^+, dimensionless wall temperature, $(T_w \rho C_p u_\tau)/q_w$;
- u, velocity (average of turbulent fluctuations) [m s^{-1}];
- u^+, dimensionless velocity, u/u_τ;
- u_m, average velocity in pipe [m s^{-1}];
- u_m^+, dimensionless average velocity, u_m/u_τ;
- u_τ, friction velocity, $(\tau_w/\rho)^{1/2}$ [m s^{-1}];
- y, coordinate distance normal to wall [m];
- y^+, dimensionless distance from the wall, $(yu_\tau)/\nu$;
- y_B, coordinate of point B (Fig. 3) [m];
- y_B^+, dimensionless coordinate of point B, $(y_B u_\tau)/\nu$;
- y_m, distance from wall at which $u = u_m$ and $T = T_m$ [m];
- y_m^+, dimensionless y_m, $(y_m u_\tau)/\nu$.

Greek symbols

- α, thermal diffusivity, $k/(\rho C_p)$ [m^2 s^{-1}];
- α_ε, total turbulent heat diffusivity, $\alpha + \varepsilon_H$ [m^2 s^{-1}];
- Δu^+, shift of logarithmic layer, equation (10);
- ε_H, turbulent heat exchange coefficient [m^2 s^{-1}];
- ε_M, turbulent momentum exchange coefficient [m^2 s^{-1}];
- μ, dynamic viscosity [kg m^{-1} s^{-1}];
- ν, kinematic viscosity, μ/ρ [m^2 s^{-1}];
- ν_{H_2O}, kinematic viscosity of water [m^2 s^{-1}];
- ν_ε, total turbulent momentum diffusivity, $\nu + \varepsilon_M$ [m^2 s^{-1}];
- ρ, density [kg m^{-3}];
- τ, shear stress [N m^{-2}];
- τ_w, wall shear stress [N m^{-2}];
- $\tau_{w/0}$, wall shear stress at onset of drag reduction [N m^{-2}].

1. INTRODUCTION

IN THE last decade considerable attention has been paid to the field of non-Newtonian fluids in general and in particular to a special category of these fluids, the dilute polymer solutions of the drag-reducing type. These fluids are of great interest in many applications as they frequently lead to striking reductions in friction and heat transfer as well as in mass transfer.

These characteristics may be of importance in a number of applications including for example pipe-line transport, drag reduction for ships and submarines, firefighting, oil well drilling, and irrigation. Less frequently mentioned but perhaps even more important are industrial processes treating fluids which naturally exhibit strong non-Newtonian behavior such as fibers suspensions, pastes and gums. Such substances may well have to be processed in the preparation of foods or the manufacture of certain chemical products.

The complete and detailed description of the interaction of the molecules or fibers with the flow is, of course, most complex and even a complete formal solution may not always be directly suitable for engineering use, because it may require detailed information on the behavior of the molecules, information which in practice may not really be available.

These considerations have led us to limit our goal to developing a method by which heat transfer and friction coefficients may be predicted for pipes of any size, on the basis of test data obtained in a single pipe. This approach is to some extent equivalent to the common practice of presenting friction and heat transfer coefficients for smooth tubes in terms of Re and Pr. The data for these presentations are also obtainable from tests in a single pipe, which, of course, reduces the required experimental work tremendously. Nevertheless, the proposed approach will still be applicable only for a given solution, that is a solution characterized by such factors as the type of polymer, concentration, and the state of degradation.

2. SUMMARY OF PREVIOUS WORK

Polymer solutions of the drag-reducing type have been studied intensively, and are covered by an extensive literature. For a basic approach of the problem, we refer the reader to the reviews [1, 2] for friction and heat transfer [3, 4].

The drag-reduction phenomena can be described briefly as follows. The Newtonian fluids can be adequately represented by the well-known universal laws

$$C_F = \frac{16}{Re} \quad (1)$$

for laminar flow [curve (1), Fig. 1] and

$$C_F^{-1/2} = 4.0 \log_{10}(Re\, C_F^{1/2}) - 0.4 \quad (2)$$

for turbulent flow [curve (2), Fig. 1].

This is not the case for viscoelastic drag-reducing fluids however. In fact the typical friction curve for the latter will be located in a domain bounded by the Newtonian friction law on the upper side and by the so-called 'maximum drag-reduction asymptote' on the lower side [Virk's asymptote, curve (3), Fig. 1]. Note that in Fig. 1 as well as in the subsequent development, we have used a simplified Reynolds number as defined for Newtonian fluids. The extension to a Reynolds number corrected on the basis of a 'power law' [5, 6] should present little difficulty as the method remains unchanged in that case. Also, the correction will most probably be small for the dilute solutions of polymers in a Newtonian solvent generally used for drag-reduction purposes. The experimental asymptote has been found to be remarkably insensitive to polymer nature, concentration and solvent, constituting a seemingly 'absolute' limitation to the decrease in friction made possible by the presence of a drag-reducing agent. Virk's equation [2] for the asymptote is

$$C_F^{-1/2} = 19.0 \log_{10}(Re\, C_F^{1/2}) - 32.4. \quad (3)$$

The actual position of the friction curve between those limits is unknown *a priori* and will depend on all the factors previously mentioned. An example of such a curve is shown in Fig. 1 and designated by curve (4).

In particular, it has been often noted that there is a rather strong influence of the diameter of the pipe on the friction law, all other factors being constant, as clearly illustrated in Fig. 2 based on ref. [7] whose data we will subsequently use for comparison with the values predicted from our approach.

The problem of the diameter effect is of particular importance as it would be most valuable to predict the friction (and heat transfer) in large scale pipes (which may be required in actual industrial applications) from data obtained with relatively small sizes in the laboratory. Accompanying the reduction in friction, a corresponding decrease in heat transfer takes place. The two phenomena cannot however be directly related by a simple law. The C_H vs Re curves will have for upper bound the Newtonian relationship described by the traditional Colburn analogy

$$C_H Pr^{2/3} = C_F/2 \quad (4)$$

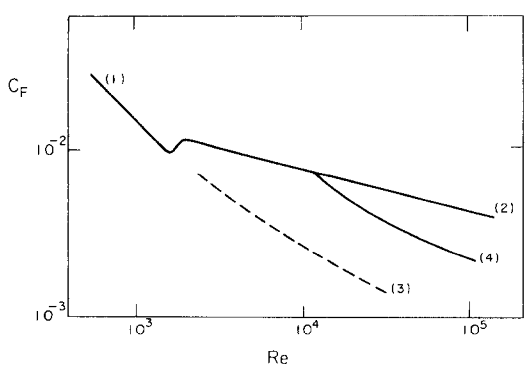

FIG. 1. Typical friction laws: friction coefficient (C_F) vs Reynolds number (Re). Curve (1): laminar flow; (2): Newtonian turbulent flow; (3): Virk's maximum drag reduction asymptote; (4): typical drag reducing fluid.

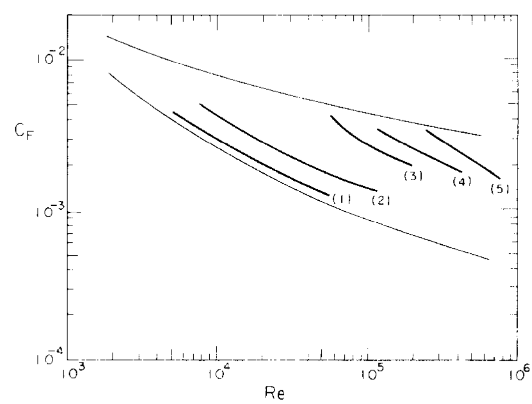

FIG. 2. The effect of diameter on friction for drag reducing fluids: friction coefficient (C_F) vs Reynolds number (Re). Solution: 500 ppm guar gum in water [7]. Curve (1): 4.1 mm dia. pipe; (2): 10 mm; (3): 52.5 mm; (4): 104.7 mm; (5): 208 mm.

and for lower bound the minimum heat transfer asymptote, an expression for which has been proposed as [4]

$$C_H Pr^{2/3} = 0.03\, Re_a^{-0.45} \quad (5)$$

where Re_a is a Reynolds number based on the apparent viscosity at the wall.

It is significant that the data and studies of heat transfer are much scarcer than the corresponding friction data for this kind of fluids. From those available, it is important to note, as has been suggested for fiber suspensions as well as for polymer solutions [4] that the often assumed Reynolds analogy ($\varepsilon_M = \varepsilon_H$) is most probably not applicable in general for any viscoelastic drag-reducing solutions. Furthermore, when taking or evaluating the experimental data, one has to take into account radical departures from Newtonian behaviour such as greatly lengthened entrance regions [4] and the anomalous readings by classical instruments (e.g. hot wire, pitot tubes). The study of heat transfer data, however, is often doubly rewarding as it may not only be helpful in providing information for design purposes, but it may also lead to a better understanding of the turbulent transport mechanism for heat and momentum transfer.

Various models have been proposed for the representation of the velocity profile in terms of the non-dimensional quantities u^+ and y^+ as used in the classical turbulent universal profile. These models are related to expressions that have been designed in the case of Newtonian fluids to represent the smooth transition between the laminar sublayer

$$u^+ = y^+, \quad (6)$$

the logarithmic profile [9]

$$u^+ = 2.5 \ln y^+ + 5.5 \quad (7)$$

and the outer wake defect law [10]. A good example is [11]

$$y^+ = u^+ + e^{-5.5K}\left[e^{Ku^+} - 1 - Ku^+ - \frac{(Ku^+)^2}{2} - \frac{(Ku^+)^3}{6}\right] \quad (8)$$

with $K = 0.4$.

3. THE DIAMETER EFFECT ON THE FRICTION COEFFICIENT

3.1. *The velocity profile*

In the present proposed approach, we will, for the sake of simplicity, use Virk's 3-layers model [2] which consists of the classical viscous sublayer [equation (6), layer 1 in Fig. 3], an 'ultimate' (or 'asymptotic') profile

$$u^+ = 11.7 \ln y^+ - 17.0 \quad (9)$$

(layer 2, Fig. 3) and a logarithmic layer

$$u^+ = 2.5 \ln y^+ + 5.5 + \Delta u^+ \quad (10)$$

(layer 3, Fig. 3). The logarithmic portion will be parallel to the Newtonian one (layer 4, Fig. 3) but

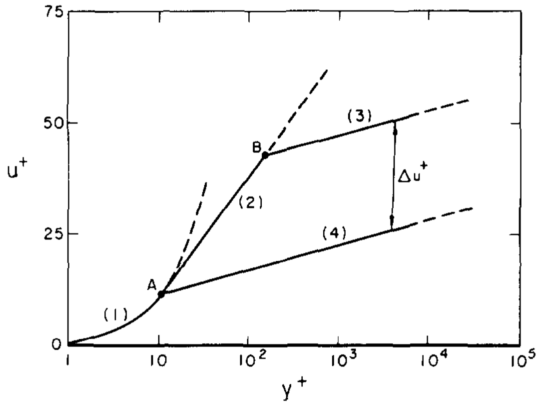

FIG. 3. Virk's velocity profile model: Dimensionless law of the wall velocity ($u^+ = u/u_\tau$) vs dimensionless distance from the wall ($y^+ = (yu_\tau)/\nu$). Curve (1): viscous sublayer; (2): Virk's elastic sublayer (3): logarithmic layer; (4): Newtonian logarithmic layer.

displaced by an amount Δu^+ which is assumed to be a function of the nature of the polymer solution, its concentration, state of degradation, flow conditions etc. Some authors have proposed that the logarithmic portions of the velocity profiles are not exactly parallel to each other and certain corrections have been suggested [12]. These are generally small, however, and we will neglect them in this first approach. We will also neglect the outer wake layer as is often done for pipe flow without adverse pressure gradient, and simply suppose that the logarithmic layer extends to the center of the pipe. We will assume that those conditions exist for the flow of our solutions and re-examine this point as we continue with the development.

The limits of the different layers are then: the triple intersection between the viscous laminar sublayer, the asymptotic profile and the Newtonian logarithmic profile (point A in Fig. 3), and the intersection of the ultimate profile with that of the central core (point B). The triple intersection (point A) is approximated by $y^+ = 12$, and point B is a function of the displacement Δu^+ of the logarithmic portion of the velocity profile with respect to the Newtonian one. This intersection is determined by

$$y_B^+ = \exp\left(\frac{\Delta u^+ + 22.5}{9.2}\right). \quad (11)$$

We will hereafter consider the increment Δu^+ as a typical number characterizing the degree, or in a sense the effectiveness, of the drag reduction. Indeed, if $\Delta u^+ = 0$, the profile collapses to the classical Newtonian one and if Δu^+ is such that $y_B^+ > R^+$, (R^+, non-dimensionalized radius), the profile will consist only of the laminar sublayer and the asymptotic interactive layer. In that case, one would expect to obtain the case defined by Virk's asymptote.

The parameters governing Δu^+ may be derived by following general dimensional analysis and the concepts of the law of the wall. The quantity Δu^+ should then depend on the type and condition of the polymer described by P and the concentration C. Appropriate forms of this parameter P could be $(u_\tau L)/\nu$ or $u_\tau^2 T/\nu$ where L is a characteristic length of the polymer and T a characteristic time. Many studies have been dedicated to finding expressions for L or T in terms of classical rheological parameters for the polymer solution such as molecular weight, number of chain links in the macromolecules, intrinsic viscosity, radius of gyration or relaxation times. For the purpose of the present study as outlined in the introduction, however, L or T may be regarded as fixed quantities for any particular solution. As a consequence Δu^+ becomes a function of u_τ only.

Making use of the velocity profiles as illustrated in Fig. 3, it is now possible to integrate numerically these profiles to find a relationship between C_F, Re and Δu^+.

Comparing these calculated values of C_F and Re to the corresponding measured values, the appropriate Δu^+ can be determined. Since for a given pipe C_F and Re also fix the value of u_τ, a relation between u_τ and Δu^+ is established. Through repeated tests in the same pipe, the desired range of Δu^+ vs u_τ may be established for each solution. Thus a curve of Δu^+ vs u_τ may be prepared which may be regarded as a basic characteristic of the particular solution.

3.2. *Numerical integration of the velocity profiles*

The steps outlined in Section 3.1 will now be described in some more detail.

Integrating the velocity from the wall ($y = 0$) to the centerline ($y = D/2$), we define an average velocity

$$u_m = \frac{4}{\pi D^2} \int_0^{D/2} 2\pi \left(\frac{D}{2} - y\right) u \, dy \qquad (12)$$

and, using the usual relations

$$u_m^+ = (2/C_F)^{1/2}, \qquad (13)$$

$$u_\tau = (\nu/D)\, Re\, (C_F/2)^{1/2} \qquad (14)$$

with

$$Re = (\rho u_m D)/\mu \qquad (15)$$

we find

$$C_F = 2\left[\frac{8}{D^2}\frac{\nu^2}{u_\tau^2} \int_0^{R^+} (R^+ - y^+) u^+ \, dy^+\right]^{-2} \qquad (16)$$

and

$$Re = \frac{8}{D}\frac{\nu}{u_\tau} \int_0^{R^+} (R^+ - y^+) u^+ \, dy^+, \qquad (17)$$

equations which give us C_F and Re in terms of u_τ and Δu^+. The value of Δu^+ appears through the logarithmic velocity profile expression and in the determination of the intersection of the asymptotic and logarithmic layers.

Carrying out the computations as indicated by equations (16) and (17) we obtain a series of curves for C_F vs Re, each curve corresponding to a different value of Δu^+. The results are shown in Fig. 4. These curves represent the relationship between C_F, Re and Δu^+ which was mentioned in Section 3.1, and which for convenience we might call the 'general C_F–Re–Δu^+' curve.

Any point on these curves is representing, for that particular 'effectiveness of drag reduction' (i.e. given Δu^+), a certain wall shear stress for a known diameter and viscosity, as

$$\tau_w = \rho[(\nu/D)\, Re (C_F/2)^{1/2}]^2. \qquad (18)$$

We have represented only the turbulent flow region since, for the type of fluids under consideration, drag reduction is known to be relevant only to that case.

It is interesting to note the very smooth tangential blending of the constant Δu^+ curves with the maximum drag reduction asymptote. This corresponds to the transition from the asymptotic to the logarithmic layer of the velocity profile.

It is also apparent that, unless u_τ and Δu^+ are such that $R^+ < y_B^+$ (i.e. the flow is still in the region of the drag reduction asymptote), the logarithmic part of the profile very soon exerts a major influence on the Re–C_F curves, as the parallelism to the Newtonian law seems to imply.

It is important to recall that for different diameters, the same value of u_τ will occur at different positions on the curve for a constant Δu^+, thus determining different pairs of the values C_F–Re. Indeed, we know that for the same Re, a given solution in different diameters of pipe will show different values of C_F (the so-called 'diameter effect').

As mentioned before, it is believed that for a given solution there is a unique relationship between u_τ and Δu^+. The value of u_τ will then be sufficient to describe the velocity in the region close to the wall, which is the one probably most responsible for the phenomena considered here. A similar proposition has been well

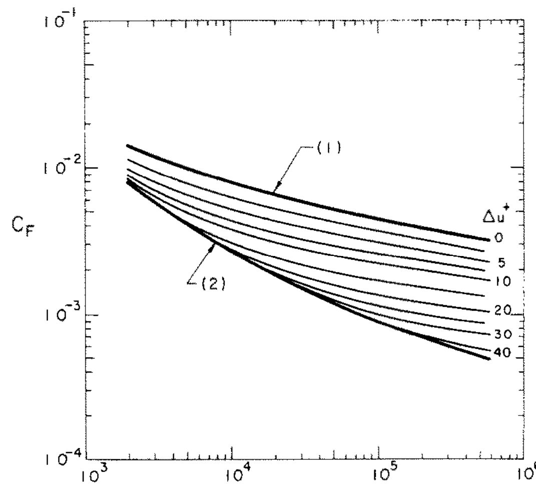

FIG. 4. General C_F–Re–Δu^+ graph (turbulent flow): Friction coefficient (C_F) vs Reynolds number (Re) for various values of Δu^+, (shift from Newtonian logarithmic velocity profile). Curve (1): Newtonian turbulent friction law; Curve (2): Virk's asymptote for maximum drag reduction.

demonstrated by the success of the classical Newtonian universal velocity profile ('law of the wall'). Thus, if the assumption that the wall region effects are predominant is correct, u_τ should be adequate to describe the whole flow and Δu^+ should be only weakly dependent on the diameter. Indeed, this has been indicated experimentally.

It is now possible therefore, after experimental measurements of the C_F vs Re law in a single pipe for a particular solution, to plot these results on our general C_F–Re–Δu^+ graph and to associate a value of Δu^+ with every combination of C_F–Re, that is for every u_τ [equation (14)]. That one-to-one relationship between Δu^+ and u_τ may in fact be regarded as a principal characteristic of a given polymer solution, as pointed out earlier.

3.3. *Prediction of the friction coefficients for different diameters*

The next step now is to apply the previous computation so as to be able to predict for a given solution the drag reduction in a pipe of any diameter from data taken in a single pipe (usually a size conveniently handled in the laboratory). It is important to repeat at this point that we are assuming that the solution to be considered in a pipe of arbitrary size will in all respects be the same as that in the test pipe.

Measurement in a test pipe of a given diameter will, by the procedure explained in the previous section, give us the relation between Δu^+ and u_τ for that particular solution.

The basic assumption we will use is that, as has been suggested before, this relationship Δu^+–u_τ is fairly independent of the diameter of the pipe for a given solution. Experiments have shown that this proposition is acceptable [13]. This assumption, as well as other types of correlations [14–16] have been used, and studies have been conducted [17–20] in an attempt to isolate and understand the nature of the diameter effect.

Using the 'general C_F–Re–Δu^+' graph (Fig. 4) together with the appropriate relationship between u_τ and Δu^+ which is applicable to the solution in question, it is now possible to predict the friction coefficient for the flow in a pipe of any desired diameter.

The computations can be summarized as follows:

Select an arbitrary C_F corresponding to the Re desired for the pipe under consideration.
Compute the associated u_τ [equation (14)].
Evaluate Δu^+ from the experimental graph Δu^+–u_τ.
For the same Re, locate the pair of values C_F–Re specified by the value of Δu^+ on the 'general C_F–Re–Δu^+' graph (Fig. 4).
Find the corresponding value of C_F. This is a new estimate for C_F.
Compute a new u_τ, etc., until the values of C_F converge to the one which then becomes our prediction for the new pipe at the specified Re.

The same procedure for different Re will give us a complete relationship between C_F and Re for that given pipe. Note that the process usually converges rapidly and 2 or 3 iterations are generally enough for each point.

4. THE 'DIAMETER EFFECT' ON THE HEAT TRANSFER COEFFICIENT

4.1. *Basic relationships*

The usual turbulent relations for shear flow may be expressed as

$$\frac{\tau}{\rho} = (\nu + \varepsilon_M)\frac{du}{dy} \tag{19}$$

and

$$q/(\rho C_p) = -\left[\frac{k}{\rho C_p} + \varepsilon_H\right]\frac{dT}{dy}. \tag{20}$$

Now, with

$$T^+ = T/[q_w/(\rho C_p u_\tau)] \tag{21}$$

and

$$\nu_\varepsilon = \nu + \varepsilon_M, \tag{22}$$

$$Pr_\varepsilon = \frac{\nu + \varepsilon_M}{\alpha + \varepsilon_H}, \tag{23}$$

$$\alpha = \frac{k}{\rho C_p}, \tag{24}$$

if we assume fully developed flow, no viscous dissipation, no axial conduction and similar variations of τ/τ_w and q/q_w, we find

$$\frac{dT^+}{dy^+} = -Pr_\varepsilon\frac{du^+}{dy^+}. \tag{25}$$

We can then integrate from $y^+ = 0$ to $y^+ = y_m^+$ where y_m^+ is the position of the average velocity u_m^+ and is also assumed to be corresponding to the average temperature T_m^+ (this should not introduce a large error for smooth tubes).

Let

$$C_H = -\frac{q_w}{\rho C_p u_m (T_m - T_w)}. \tag{26}$$

Then [21]

$$T_m^+ - T_w^+ = -(C_F/2)^{1/2}(1/C_H). \tag{27}$$

Also, with

$$u_m^+ = \int_0^{y_m^+}\left[\frac{du^+}{dy^+}\right]dy^+ \tag{28}$$

we finally find that the combination of terms which is sometimes called the Dipprey number is given by

$$[(0.5C_F/C_H) - 1](C_F/2)^{-1/2} = \int_0^{y_m^+}(Pr_\varepsilon - 1)\left(\frac{du^+}{dy^+}\right)dy^+ \tag{29}$$

Note that we did not need to make any assumption regarding the value of Pr_ε and that the Reynolds analogy, in particular, did not have to be introduced.

Supposing again, as mentioned earlier in Section 3.1, that the polymer solution can be described by the parameters C and P, for a given solution the phenomena will be characterized by u_τ only. We can write then

$$\frac{du^+}{dy^+} = f_1(C, P, y^+) = f'_1(u_\tau, y^+). \quad (30)$$

Assuming also as before a unique relationship between Δu^+ and u_τ for each solution, it follows that

$$y^+_m = f_2(\Delta u^+, u_\tau) = f'_2(u_\tau). \quad (31)$$

For heat transfer, the Prandtl number of the solution will also have to be included as a parameter. The way in which P has been defined, the possibility that it depends on temperature must be considered too. A given temperature, however, will fix the value of Pr and the dependence on temperature of P, so that for a particular solution and temperature, we have

$$Pr_\varepsilon = f_3(Pr, C, P, y^+) = f'_3(u_\tau, y^+). \quad (32)$$

Finally, after integration with respect to y^+ in equation (29), we find

$$[(0.5C_F/C_H) - 1](C_F/2)^{-1/2} = F(u_\tau). \quad (33)$$

We can thus with the experimental data for C_F–Re and C_H–Re in a single pipe, compute the previous function [equation (33)] which is a characterization of the combined heat transfer and friction reduction induced by that particular solution.

The procedure of predicting heat transfer coefficients for pipes of different diameters may now be summarized.

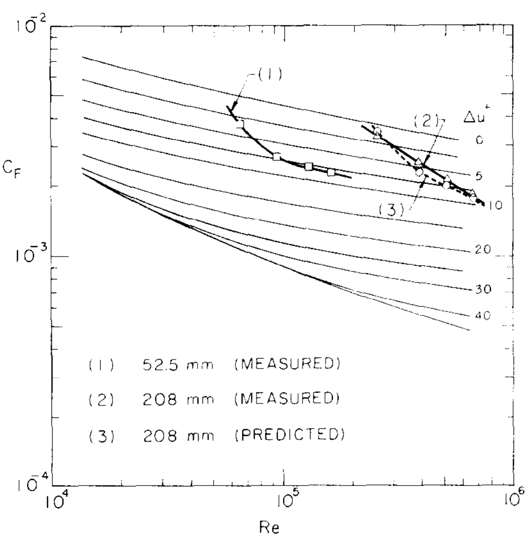

FIG. 5. Prediction of the diameter effect on friction: Friction coefficient (C_F) vs Reynolds number (Re). Solution: 500 ppm guar gum in water [7]. Curve (1): experimental data for 52.5 mm pipe; Curve (2): experimental data for 208 mm pipe; Curve (3): prediction for 208 mm pipe on basis of 52.5 mm data.

After obtaining friction and heat transfer data experimentally in a single test pipe, we can predict the C_F–Re law for another diameter by first computing the Δu^+–u_τ function as explained in Section 3.

We next also compute

$$[(C_F/2C_H) - 1]/(C_F/2)^{1/2} = F(u_\tau) \quad (34)$$

from those data, where $F(u_\tau)$ is a function of u_τ only and is not directly dependent on the diameter. For a desired Re and the predicted C_F, we can compute u_τ [equation (14)]. With these values of u_τ and C_F, C_H is obtained from the previously found relation [equation (34)], which will usually be given in graphical or numerical form.

5. EXAMPLES

5.1. *Prediction of the friction coefficient*

Let us try to predict friction coefficients for a pipe of 208 mm dia from the experimental data for a 52.5 mm one, for a guar gum solution of 500 ppm in water. The experimental data are taken from ref. [7]. In Fig. 5 we have plotted the experimental data for the 52.5 mm pipe on the general 'C_F–Re–Δu^+' graph, the curve is designated (1). From the intersection of the experimental curve with the constant Δu^+ curves, we can compute the relation Δu^+ vs u_τ (Fig. 6). In so doing we have used the expression

$$\nu = \nu_{H_2O}(1 + 4.73\,10^{-4}\,C_1^{1.157})$$

(where C_1 is the concentration in ppm) for the viscosity.

This curve of Δu^+ vs u_τ is considered to be a unique characteristic of this solution. The shape of this curve is also typical in that it shows a rather rapid increase in Δu^+ after u_τ reaches the 'onset' value (the minimum for which any drag reduction is noted) and more gradual increase of Δu^+ for large values of u_τ.

Incidentally this relationship between Δu^+ and u_τ may be used to address a problem often encountered by engineers working in this field. The fluids we are concerned with do degrade with use and there have been difficulties in quantifying in a convenient way the extent of degradation they experience. Also sometimes the relative effectiveness of different additives has to be

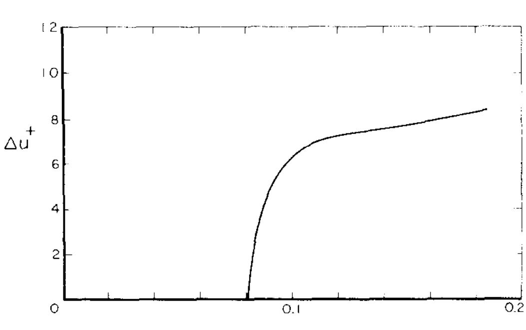

FIG. 6. Characteristic curve for drag reducing fluid: Shift from Newtonian logarithmic velocity profile (Δu^+) vs friction velocity [$u_\tau = (\tau_w/\rho)^{1/2}$]. Solution: 500 ppm guar gum in water [7]. Computed from data in 52.5 mm tube.

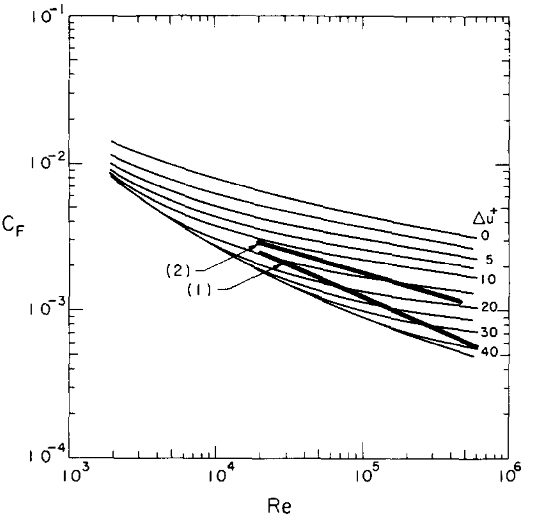

FIG. 7. Prediction of the diameter effect on friction: Friction coefficient (C_F) vs Reynolds number (Re). Solution: 50 ppm polyethylene oxide in water, Pr = 6.16, [22]. Curve (1): experimental data for 0.95 cm dia. pipe; Curve (2): prediction for 5 cm pipe.

evaluated. It may be suggested that the use of the Δu^+-u_τ relationship might prove convenient for such purpose by enabling us to compute typical ratios of wall shear stress at onset and comparisons of Δu^+ for given u_τ.

Following the steps outlined in Section 3.3, we may now predict the curve of C_F vs Re for a 208 mm pipe with the same gum solution [curve (3), Fig. 5]. We have plotted for comparison the actually measured data for a 208 mm pipe as given in ref. [7] (curve 2, Fig. 5).

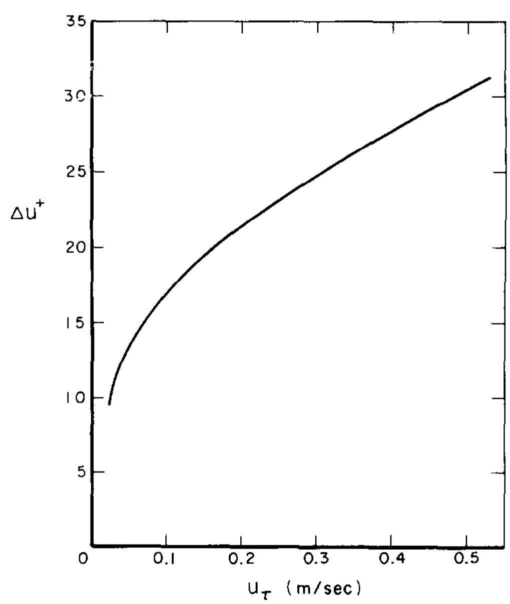

FIG. 8. Characteristic curve of drag reduction: Shift from Newtonian logarithmic velocity profile (Δu^+) vs friction velocity [$u_\tau = (\tau_w/\rho)^{1/2}$]. Solution: 50 ppm polyethylene oxide in water. Pr = 6.16 [22]. Computed from data in 0.95 cm tube.

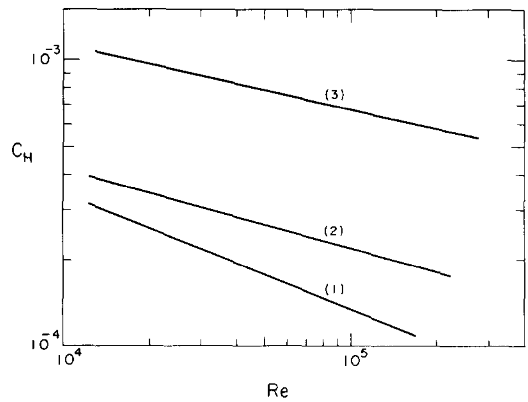

FIG. 9. Prediction of the diameter effect on heat transfer: Heat transfer coefficient (C_H) vs Reynolds number (Re). Solution: 50 ppm polyethylene oxide in water Pr = 6.16 [22]. Curve (1): experimental data for 0.95 cm pipe; Curve (2): prediction for 5 cm pipe; Curve (3): Newtonian heat transfer law.

The agreement is rather good, suggesting that the proposed method might be based on a reasonable concept of the transfer processes.

5.2. *Prediction of the heat transfer coefficient*

We have not been able so far to find suitable data in the literature mentioning explicity heat transfer results for different diameters and providing all the necessary information. We were thus not able to actually compare the prediction for heat transfer with actual experimental data.

However, for a better illustration of the method, we will use here data from ref. [22]. From measurements of a solution of 50 ppm of polyethylene oxide in water in a 0.95 cm dia. tube, at a temperature corresponding to Pr = 6.16, we will try to predict friction and heat transfer for a hypothetical 5 cm dia. tube in the same conditions.

In Fig. 7, we show the measured friction data for a

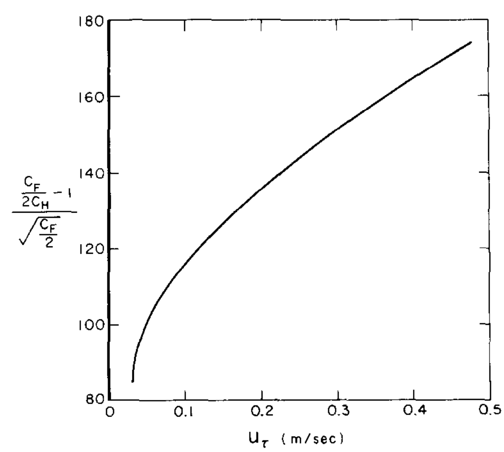

FIG. 10. Characteristic combined heat transfer and friction curve for drag reducing fluid: Dipprey number $\{[(0.5C_F/C_H) - 1]/(C_F/2)\}^{1/2}\}$ vs friction velocity [$u_\tau = (\tau_w/\rho^{1/2})$]. Solution: 50 ppm polyethylene oxide in water, Pr = 6.16 [22]. Computed from data in 0.95 cm tube.

0.95 cm pipe [curve (1)] and the predicted data for a 5 cm pipe [curve (2)]. The predictions were obtained as described in Section 5.1, and the Δu^+ vs u_τ curve used in the process is shown in Fig. 8.

To obtain the heat transfer coefficient, it is now first necessary to plot the parameter $\{[(0.5C_F/C_H) - 1]/(C_F/2)^{1/2}\}$ vs u_τ which can be done from the data for the 0.95 cm tube. The curve is shown in Fig. 10, with the aid of which, C_F and u_τ being already computed, the appropriate value for C_H can be easily obtained. The resulting graph of C_H vs Re for the 5 cm tube is shown in Fig. 9, together with the data for the smaller pipe. For reference the heat transfer coefficient for a Newtonian fluid with $Pr = 6.16$ [curve (3)], computed from Colburn analogy, is also shown

Although it is not possible at this time to compare these results with actual data, they are likely to give a valid estimate for the illustration of the importance of the diameter effect on heat transfer, an effect usually far from negligible.

Indeed, it has been shown that the heat transfer is usually reduced even more than the friction by the drag-reducing additive. Studies have been conducted (for example [4]) to estimate the values of heat and momentum transport coefficients that would lead to the observed heat transfer and drag reduction, and it has been shown that the heat transport coefficient can be much lower close to the wall than the momentum one for certain solutions.

6. SUMMARY AND CONCLUSIONS

We have reported here a proposed method of predicting the diameter effect for drag-reducing solutions.

A simplified model of the velocity profile is assumed which includes a shift, Δu^+, of the logarithmic layer. This velocity profile is numerically integrated to compute a 'general C_F–Re–Δu^+' graph. We can then obtain for the solution considered a relationship between this shift Δu^+ and the friction velocity u_τ, using data obtained for experiments in a single pipe.

This relationship is taken as a major characteristic describing the behavior of the drag-reducing fluid and is assumed to be valid regardless of the diameter of the pipe. It is then possible to make predictions for the friction in pipes having different diameters.

Rather analogous assumptions could be made in analyzing the heat transfer problem. As a result it was shown that the Dipprey number $[(0.5C_F/C_H) - 1]/(C_F/2)^{1/2}$ for a given solution should be a function of the friction velocity u_τ only.

The use of this last function allows us to make predictions for heat transfer in a pipe of any diameter, on the basis of a set of heat transfer experiments taken in a single pipe with the fluid to be examined.

Experimental data for friction were available for comparison with the values predicted by the proposed method. The agreement was considered quite satisfactory.

REFERENCES

1. J. W. Hoyt, The effect of additives on fluid friction, *Trans. Am. Soc. Mech. Engrs*, Series D, *J. Bas. Engng* **94**, 258–285 (1972).
2. P. S. Virk, Drag reduction fundamentals, *A.I.Ch.E. Jl* **21**, 625–656 (1975).
3. Y. Dimant and M. Poreh, Heat transfer in flows with drag reduction, in *Advances in Heat Transfer*, Vol. 12, pp. 77–113 (1976).
4. Y. I. Cho and J. P. Hartnett, Non-Newtonian fluids in circular pipe flow, in *Advances in Heat Transfer*, Vol. 15, pp. 59–139 (1981).
5. A. B. Metzner and J. C. Reed, Flow of non Newtonian fluids, correlation of the laminar, transition and turbulent flow regions; *A.I.Ch.E. Jl* **1**, 434–440 (1955).
6. D. W. Dodge and A. B. Metzner, Turbulent flow of non-Newtonian systems, *A.I.Ch.E. Jl* **5**, 189–204 (1959).
7. J. P. De Loof, B. De Lagarde, M. Petry and A. Simon, Pressure drop reduction in large industrial ducts by macromolecular additives, *2nd Int. Conf. on Drag Reduction*, BHRA Pub., paper B2 (1977).
8. A. L. Moyls and R. H. Sabersky, Heat transfer and friction coefficients for dilute suspensions of asbestos fibers, *Int. J. Heat Mass Transfer* **21**, 7–14 (1978).
9. J. Nikuradse, Gesetz mässigkeiten der turbulenten strömung in glatten Rohren, *V. D. I., Forsch.* **356** (1932).
10. D. E. Coles, The law of the wake in turbulent boundary layer, *J. Fluid Mech.* **1**, 191–226 (1956).
11. D. B. Spalding, A single formula for the law of the wall, *J. Appl. Mech.* **28**, 455–457 (1961).
12. D. C. Bogue and A. B. Metzner, Velocity profiles in turbulent pipe flow; *I/EC Fundamentals* **2**, 143–149 (1963).
13. T. T. Huang, Similarity laws for turbulent flow of dilute solutions of drag reducing polymers, *Physics Fluids* **17**, 298–309 (1974).
14. J. G. Savins and F. A. Seyer, Drag reduction scale-up criteria, *Physics Fluids* **20**, S78–S84 (1977).
15. P. Katsibas, C. Balakrishnan, D. White and R. J. Gordon, Drag reduction correlations; *Int. Conf. on Drag Reduction*, September 1974, BHRA Pub., paper B2 (1974).
16. P. S. Granville, Scaling-up of pipe flow frictional data for drag-reducing polymer solutions; *2nd Int. Conf. on Drag Reduction*, BHRA Pub., paper B1 (1977).
17. R. Y. Ting, Diameter dependence on the cutoff molecular weights of drag reducing polymers; *J. Appl. Polym. Sci.* **20**, 3017–3023 (1976).
18. C. S. Wells, Use of pipe flow correlations to predict turbulent skin friction for drag reducing fluids, *J. Hydronautics* **4**, 22–26 (1970).
19. J. H. Elliott and F. S. Stow Jr., Solutions of drag reducing polymers: diameter effect and rheological properties, *J. Appl. Polym. Sci.* **15**, 2743–2748 (1971).
20. D. D. Taylor and R. H. Sabersky, Extrapolation to various tube diameters of experimental data taken with dilute polymer solutions in a smooth tube, *Lett. Heat Mass Transfer* **1**, 103–108 (1974).
21. R. L. Webb, E. R. Eckert and R. J. Goldstein, Heat transfer and friction in tubes with repeated rib roughness, *Int. J. Heat Mass Transfer* **14**, 601–617 (1971).
22. P. M. Debrule and R. H. Sabersky, Heat transfer and friction coefficients in smooth and rough tubes with dilute polymer solutions, *Int. J. Heat Mass Transfer* **17**, 529–540 (1974).

Résumé—Un profil de vitesse multi-couches est supposé exister pour les fluides du type 'réducteurs de friction' lors de leur écoulement en tube.

Le profil est charactérisé par une portion logarithmique rehaussée d'un incrément Δu^+ par rapport à celle représentant les fluides Newtoniens. Pour une certaine solution, Δu^+ est supposé être déterminé par la 'vitesse de cisaillement' u_τ.

Sur ces bases, une méthode est proposée à l'aide de laquelle il est possible de prédire l'effet d'une variation de diamètre sur les coefficients de friction et de transfert de chaleur.

EINE METHODE ZUR BESTIMMUNG DES "DURCHMESSER-EFFEKTS" BEI WÄRMEÜBERGANG UND DRUCKABFALL VON WIDERSTANDSVERMINDERNDEN FLÜSSIGKEITEN

Zusammenfassung—Die Existenz eines vielschichtigen Geschwindigkeitsprofils wird für die Rohrströmung widerstandsvermindernder Fluide angenommen. Das Profil wird durch einen logarithmischen Bereich, der um das Inkrement Δu^+ gegenüber dem für ein newton'sches Fluid geltendem Profil verschoben ist, charakterisiert. Für ein gegebenes Fluid wird angenommen, daß Δu^+ durch die Schergeschwindigkeit u_τ bestimmt wird. Auf dieser Grundlage wird eine Methode vorgeschlagen, mit deren Hilfe man den Einfluß von Änderungen im Durchmesser auf die Reibungs- und Wärmeübergangskoeffizienten bestimmen kann.

МЕТОД ПРЕДСКАЗАНИЯ "ЭФФЕКТА ДИАМЕТРА" НА ТЕПЛОПЕРЕНОС И ТРЕНИЕ ЖИДКОСТЕЙ, СНИЖАЮЩИХ СОПРОТИВЛЕНИЕ

Аннотация—Предполагается, что снижающие сопротивление жидкости имеют многослойный профиль скорости при течении в трубе. Логарифмическая часть профиля получает приращение на величину Δu^+ по сравнению с характерным для ньютоновской жидкости значением. Для рассматриваемой жидкости предполагается, что величина Δu^+ определяется скоростью сдвига u_τ. На основании этого предложен метод, позволяющий предсказать влияние изменения диаметра на трение и теплоперенос.